Section: Technical Note

Surface layer profiles of air temperature and humidity measured from unmanned aircraft

Stephen Hobbs(1*), David Dyer(1), Dominique Courault(2), Albert Olioso(2), Jean-Pierre Lagouarde(3), Yves Kerr(4), John McAnneney(3) and Jean Bonnefond(3)

[1] Cranfield University, Cranfield, Bedford, MK43 0AL, UK

[2] INRA Bioclimatologie, Site Agroparc, 84 914 Avignon, France

[3] INRA Bioclimatologie Bordeaux, Domaine de la grande Ferrade, BP 81, 33 883 Villenave d'Ornon, France

[4] CESBIO, 18, AV Edouard Belin, 31 055 Toulouse, France

*Corresponding author:

Dr. Stephen Hobbs, School of Engineering, Cranfield University, Cranfield, Bedford, MK43 0AL

Tel +44 (0) 1234 750111

Fax: +44 (0) 1234 751550

s.e.hobbs@cranfield.ac.uk

Abstract

The atmospheric surface layer couples processes in the atmosphere with those at the land surface, but is not fully understood for heterogeneous land surfaces. A small remotely piloted aircraft was flown during the ReSeDA experiment to measure profiles of heat and humidity in the surface layer near boundaries between different land cover types to study atmospheric structure over heterogeneous terrain.

The aircraft payload included sensors for temperature, humidity and position. Extensive data processing has been performed to check data quality and coordinate the datasets created (to common time and position references).

Initial results show the expected general features of the surface layer profiles of temperature and humidity and also give details of structure near field boundaries, especially where there is strong contrast in surface properties and radiative forcing. The experiments also demonstrate that unmanned aircraft are practical tools for this form of atmospheric research.

Mesures de température et d'humidité par avion télécommandé

Résumé

Les processus qui interviennent dans la couche limite de surface (CLS) entre l'atmosphère et la surface sont encore loin d'être parfaitement connus sur des surfaces hétérogènes. Un petit avion télécommandé a été utilisé dans le cadre de l'expérimentation Alpilles-ReSeDA, pour mesurer des profils de température et d'humidité

dans la CLS au niveau des transitions entre différents types de parcelles agricoles. Le but était d'étudier la structure de l'atmosphère au dessus des hétérogénéités de surface. L'avion comprenait différents capteurs pour mesurer la température, l'humidité et avoir la position géographique exacte (GPS). Des traitements ont été effectués pour vérifier la qualité des données et géoréférencer ces données sur des cartes. Les premiers résultats montrent des profils de températures et d'humidité cohérents et donnent aussi des informations sur la structure de l'atmosphère à proximité des limites des parcelles, lorsqu'il y a un fort contraste des propriétes de surface et un rayonnement élévé. Cette expérimentation démontre aussi que ce type de mesures aéroportées représente un outil intéressant et pratique pour étudier l'atmosphère.

Keywords

Atmospheric surface layer / surface heterogeneity / ReSeDA / UAV / Vaisala Humitter

couche limite de surface / ReSeDA / UAV / surface hétérogène / Vaisala Humitter

1. Introduction

The atmospheric surface layer couples the atmosphere with the Earth's surface. Over heterogeneous surfaces, widely represented globally, atmospheric structure is complex and only partially understood [5]. One of the aims of ReSeDA was to study the spatial structure of the surface layer (below 100 m) and energy fluxes between the surface and the atmosphere.

Practical means of measuring atmospheric structure are limited. Available techniques are (a) remote sensing, e.g. Raman lidar [1] or tomography [12], and (b) *in situ* measurements, either from a mobile vehicle, e.g. aircraft [2], or using a dense network of fixed masts. An uninhabited aerial vehicle (UAV) was chosen for this project because of its versatility in terms of payload, field operations and flight pattern. The objectives of the UAV flights were (1) to evaluate UAV's for ABL research, and (2) to investigate the surface layer structure near boundaries between different landcover types in various weather conditions.

The following sections introduce a sample of relevant literature, describe the experiments performed for ReSeDA in June 1997 and the sensor calibrations, summarise the results, and then discuss the findings.

2. Previous Studies

Mahrt [7] gives an excellent overview of current understanding of the structure of the atmospheric boundary layer (ABL) as it adjusts to changes in surface properties in different conditions. Two key concepts for understanding ABL structure close to the surface and the way surface fluxes aggregate are (1) the internal boundary layer - the region of the atmosphere where flow changes downwind of a surface transition to be in equilibrium with the new surface, and (2) the blending height - the height at which fluxes

from individual surface types average out and lose their horizontal variation. Kaimal and Finnigan [5] discuss internal boundary layers, and the blending height concept is examined by, for example, Schmid and Bünzli [10]. Observations of ABL structure corresponding to these concepts are difficult to obtain and were one goal of the experiments performed for ReSeDA.

Aircraft have been used as research vehicles in the atmosphere for many years. Recent developments in technology however enable small and light but very capable aircraft to be built and several have been demonstrated [3,4,6,8]. Developments in micro air vehicles may in time lead to further tools for micrometeorology. Aerosonde [3,4,8] is similar in size, mass and payload to the aeroplane used for ReSeDA but is not designed for measurements within 10 m of the surface and the airframe appears to be less robust.

3. Experiments and Aircraft

The experiments comprised a set of flights over 4 days at 3 sites in the ReSeDA area (see Table I). The aircraft was flown at 25 ms^{-1} at various heights (1-15 m) into the wind across field boundaries. Each flight lasted about 20 minutes and typically included 15 horizontal profiles.

The aircraft built for the experiments has a span of 2.5 m, mass of 15 kg, and is remotely piloted. Figure 1 shows it ready for take-off from its bungee-powered launch rail. The aircraft lands on short grass or bare soil. Reliable operation of such aircraft requires significant practical expertise.

The aircraft sensors were GPS for position (a base station GPS receiver enabled differential mode position measurements), a fine Pt wire thermometer for temperature, and a bare Vaisala Humitter (model 50-Y) for humidity. The Pt wire thermometer is used to measure relative temperature since this is more significant for atmospheric structure than absolute temperature (which could be obtained using a reference thermometer if

needed). The Pt wire sensitivity to solar radiation is <0.005 K and no shading is required. The Humitter is sensitive to insolation at low airspeeds but at 25 ms^{-1} the effect is significantly reduced. The Pt thermometer's bandwidth is estimated to be >30 Hz.

The Humitter's time response in flight is difficult to measure directly, but has been estimated by two methods: analysis of flight data and direct experiments. The Humitter has two sensor elements, one each for temperature (Pt film) and humidity (moisture absorbing polymer). The humidity measurement reported is relative humidity which depends on air temperature and absolute humidity. Direct measurements of the time constants (obtained by moving the Humitter rapidly between dry / moist and cool / warm air) give the following principal results (Humitter with silvered cap removed).

- Results showed wide scatter, and the shortest time constants measured were 2.7 s (temperature) and 0.28 s (humidity) (airflow ~3 ms^{-1}, i.e. ~10% of flight speed).
- Where both time constants could be measured, the mean ratio ($\tau_{Humidity}$ / $\tau_{Temperature}$) was 0.36 ±0.06.
- The humidity response is faster for changes in mixing ratio than temperature.

Since two different temperature sensors were carried during the flights, it is possible to compare the frequency response of the two sensors (Pt wire and Humitter). The Pt wire has a much higher bandwidth and has been used as a reference against which the transfer function for the Humitter's temperature sensor can be measured. Figure 2 shows typical results to which a first order time constant model has been fitted. The time constant of the Humitter's temperature sensor estimated by this method is 1.86 s.

Combining these results suggests that the effective time constant for the humidity measurements will be 1.86 x 0.36 = 0.67 s (this may be conservative by a factor of 2 since values less than half this have been measured directly). The corresponding bandwidth is $1 / 2 \pi \tau$ = 0.24 Hz which corresponds to a length of ~100 m at flight speed.

Each sensor's readings were logged at 16 sample s^{-1} with 2^{nd} order anti-aliasing filters (the GPS measurement rate is 1 Hz). The Pt wire temperature sensor data thus have an effective bandwidth of 8 Hz, corresponding to structures of ~3 m at flight speed. Regulations for operating remotely piloted aircraft and for data telemetry must be complied with.

4. Results

Five datasets were recorded: (1) payload sensors (temperature, humidity), (2) aircraft GPS position, (3) reference station GPS data, (4) video log of the flights, and (5) site data (feature locations and surface elevation) from maps. Data processing was a major task (about 50% of project effort) and comprised checking the data quality, GPS data analysis, and producing regular coordinated datasets. The full datasets and supporting documentation are available from the ReSeDA database (www.avignon.inra.fr/reseda).

Figures 3 and 4 show sample results. Figure 3 has subplots of data from Flight 4 (overcast weather) showing (a) the aircraft height as a function of time and (b) its horizontal position (when below 15 m) over the site relative to field boundaries. The aircraft flew between fields with bare soil (Field 121) and harvested alfalfa (Field 203, coordinates are relative to a local site origin). The other two parts of the figure show the measured (c) temperature relative to the mean temperature over the whole flight, showing a lapse rate of -10 K km^{-1} indicative of neutral stability (consistent with the Pasquill-Gifford stability class estimated from standard meteorological data), and (d) absolute humidity, with scatter of ~5% and some near-surface enhancement.

Figures 4 (a) and (b) show example horizontal profiles of temperature and humidity from Flight 9 (during which there was strong insolation and a surface wind of 4-5 ms^{-1}). These data are illustrative, and require significant additional information for rigourous analysis and interpretation. It appears that a temperature contrast exists at all three heights

plotted, and that the peak temperature moves downwind with increasing height (displaced ~50 m per 20 m height increase). For humidity the strongest contrast is close to the surface but structure is apparently still detectable at 50 m (land cover upwind and the exact flight path followed require further investigation). These results show that the aircraft with even this basic level of instrumentation is able to detect structure and influences of the surface on the atmosphere. More detailed analysis is possible using the data to obtain parameters such as the structure constant, from which inferences can be made concerning heat fluxes.

5. Discussion

The key findings of the research to date are the experience of using a UAV for near-surface measurements and the observations of contrast in atmospheric properties near boundaries in various conditions (weather and landcover).

5.1 Unmanned Aircraft

The experiments involved UAV operations at three sites; one vehicle was used to transport all equipment and no local support facilities were required. The aircraft was operated without major damage (although the Pt wire temperature sensor did require replacement). Bare soil and short grass were the easiest surfaces to operate from - long grass damages sensors and decelerates the aircraft abruptly on landing. A skilled pilot was able to fly the aircraft using visual contact to a range of about 1 km, and close to the surface (height < 3 m) to a radius of 200 m. Pilot concentration and the aircraft's fuel load limited safe flight duration to about 20 min. Flights were repeated at intervals of about 2 hr. An autonomous aircraft would be capable of more intensive operations and would be well-suited to routine measurements but a human pilot is generally better able to adapt to the evolving requirements which characterised these exploratory flights.

To maximise scientific yield the experimenter needs to assess sensor data in (near) real-time to detect faults and exploit opportunities. Aircraft can be used most effectively when part of a coordinated experiment with clear objectives. Other reports of similar UAV operations are rare, but Shields and Testa [11] provide useful practical details.

5.2 ABL Structure

Structures compatible with the internal boundary layer concept have been observed, as has some reduction in horizontal heterogeneity with height. The strongest contrast was observed in unstable conditions with differing surface cover (e.g. dry vs irrigated), whereas in neutral conditions little contrast was observed at any boundary. This pattern is consistent with the literature. The analysis performed is largely qualitative, and more rigourous analysis of the data requires results from quantitative models of ABL structure and may need more extensive experiments.

We note that the conditions in which the strongest contrast was observed (Flights 9,10) also corresponded to the case where there was the most significant physical barrier between fields (a dyke with shrubs rather than wire fence or narrow strip of rough ground). If this helped provide a steadier internal boundary layer it would have made the contrast easier to observe in these experiments where several passes during a period of 20 minutes are used to investigate structure.

6. Conclusions

The experiments demonstrate that a UAV is capable of observing ABL surface layer structure near landcover boundaries, and is a practical research platform. Good sensor characterization, and good quality, timely, payload data properly coordinated with wider experiment data in a convenient format are important for scientific applications. For the atmospheric stability conditions (neutral and unstable) and field sizes (a few hundred

metres) experienced, the horizontal contrast in the ABL below 30 m was strongest in unstable conditions.

7. Acknowledgements

The work was funded by Cranfield University and the EC. Without the commitment of UAV engineers at Cranfield the experiments would not have been possible within the short timescale available. The support of the whole ReSeDA team and the referees' constructive comments are much appreciated.

8. References

[1] Cooper, D.I., Eichinger, W.E., Holtkamp, D.B., Karl, R.R., Quick, C.R., Dugas, W., and Hipps, L., Spatial variability of water vapor turbulent transfer within the boundary layer. Boundary-Layer Meteorology, vol 61, pp 389-405, 1992.

[2] Frech, M., and Jochum, A., The evaluation of flux aggregation methods using aircraft measurements in the surface layer. Agricultural and Forest Meteorology, vol 98-99, pp 121-143, 1999.

[3] Holland, G.J., McGeer, T., and Youngren, H., Autonomous aerosondes for economical atmospheric soundings anywhere on the globe. Bulletin of the American Meteorological Society, vol 73(12), pp 1987-1998, Dec 1992.

[4] Holland, G.J., Webster, P.J., Curry, J.A., Tyrell, G., Gauntlett, D., Brett, G., Becker, J., Hoag, R., and Vaglienti, W., The Aerosonde robotic aircraft: a new paradigm for environmental observations. Bulletin of the American Meteorological Society, vol 82(5), pp 889-901, May 2001.

[5] Kaimal, J.C., and Finnigan, J.J., Atmospheric boundary layer flows, their structure and measurement. Oxford University Press, 1994.

[6] Kukharets, V.P., and Tsvang, L.R., Radio-controlled aircraft to investigate atmospheric turbulence. Proc. 9th Symposium on Met. Observ. and Instrumentation, American Meteorological Society, pp 529-530.

[7] Mahrt, L., Surface heterogeneity and vertical structure of the boundary layer. Boundary Layer Meteorology, vol 96 (1/2), pp 33-62, August 2000.

[8] McGeer, T., and Holland, G.J., Small autonomous aircraft for economical oceanographic observations on a wide scale. Oceanography, vol 6(3), pp 129-135, 1993.

[9] Pasquill, F., and Smith, F.B., Atmospheric Diffusion, 3rd Edition. Ellis Horwood Limited, Chichester, 1983.

[10] Schmid, H.P., and Bünzli, D., The influence of surface texture on the effective roughness length. Quarterly Journal of the Royal Meteorological Society, vol 121(A), no 521, pp 1-22, Jan 1995.

[11] Shields, E.J., and Testa, A.M., Fall migratory flight initiation of the potato leafhopper, *Empoasca fabae* (Homoptera: Circadellidae): observations in the lower atmosphere using remote piloted vehicles. Agricultural and Forest Meteorology, vol 97, pp 317-330, 1999.

[12] Ziemann, A., Arnold, K., and Raabe, A., Acoustic travel time tomography as a remote sensing method for the characterisation of natural surfaces. Proceedings EGS General Assembly, Nice, April 2000, Geophysical Research Abstracts, Vol 2, 2000. (ISSN 1029-7006)

Figure legends

Figure 1. The aircraft (length 2 m, span 2.5 m) ready for take-off on its launch rail. The temperature and humidity sensors are mounted on the white hatch between the nose and the wing.

Figure 2. Transfer function for the Humitter temperature sensor calculated using data from Flight 10 (solid line) by comparing spectra from the Humitter and a high bandwidth temperature sensor (Pt wire). The dashed line shows a least squares fit of a first order time constant model (τ = 1.86 s).

Figure 3. Flight 4 summary plots showing the aircraft's position and payload data. Subfigure (b) shows the aircraft's position relative to field boundaries. The wind was from the South-East (parallel to the plotted aircraft tracks). The boundary crossed at low level was between bare soil (Field 121, upwind) and harvested alfalfa and wheat (Fields 203,202 downwind). In subfigures (c) and (d) a point is plotted for each 0.5 s of the flight.

(a) Aircraft height variation during the flight.

(b) Field boundaries and aircraft track (track shown only when height < 15 m, aircraft crosses boundary at 610,710).

(c) Temperature variation as a function of height (relative to mean over whole flight)

(d) Measured absolute humidity height profile

Figure 4. Horizontal profiles of temperature and humidity (averaged over 50 m horizontally and 0-20 m, 20-40 m, and 40-60 m vertically, using all available data) relative to the means during the whole of flight 9. An irrigated meadow was upwind of the boundary and a dry fallow field downwind.

(a) Temperature relative to the mean as a function of distance upwind of field boundary at heights of 10, 30 and 50 m.

(b) Humidity relative to the mean as a function of distance upwind of field boundary at heights of 10, 30 and 50 m.

Tables

Flight	Site	Date	Take-off UT	Length s	Stability	Remarks
2	l'Ermite (43° 40'N, 4° 44'E)	20/6/97	14:19:02	809	A/B	Grass / wheat boundary
3			16:59:56	781	A/B	
4	Alpilles (43° 48'N, 4° 45'E)	21/6/97	14:42:49	779	C/D	Overcast
5			15:51:34	946	C/D	Soil / wheat / alfalfa boundaries
6		22/6/97	12:57:12	1195	A	Drying after rain
7			15:07:49	1095	B/A	Bare soil / wheat boundary
8			17:43:25	848	C	
9	La Crau (43° 37'N, 4° 41'E)	23/6/97	10:58:18	748	B	Meadow / fallow boundary
10			12:51:40	855	B	

Table I. UAV flights for the ReSeDA experiments in June 1997. Atmospheric stability is described using the Pasquill-Gifford stability classes [9], where A and B are unstable, C is neutral stability, and D is stable. More details are available from the ReSeDA database. Flights consisted of 10-15 circuits with low passes into wind perpendicular to field boundaries at heights up to 15 m; the aircraft returned to the downwind side of the boundary at about 50 m. (Flight 1 was a test flight prior to the experiments and is omitted from the table.)

Figures

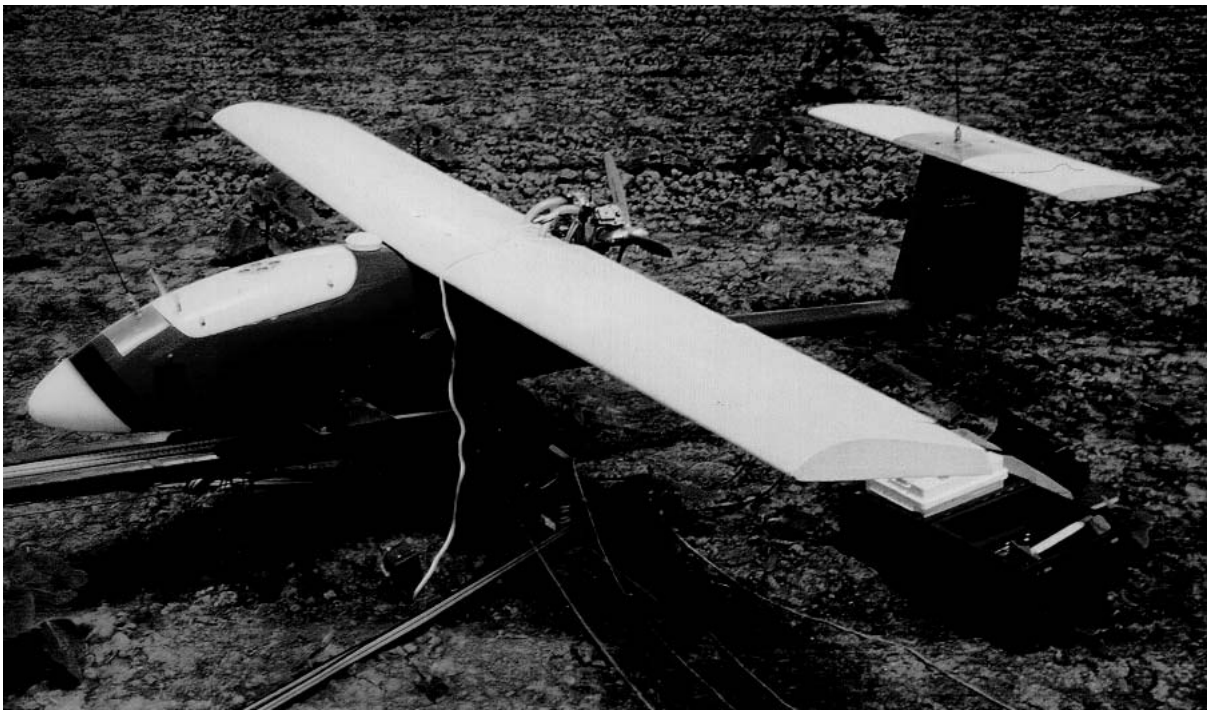

Figure 1. The aircraft (length 2 m, span 2.5 m) ready for take-off on its launch rail. The temperature and humidity sensors are mounted on the white hatch between the nose and the wing.

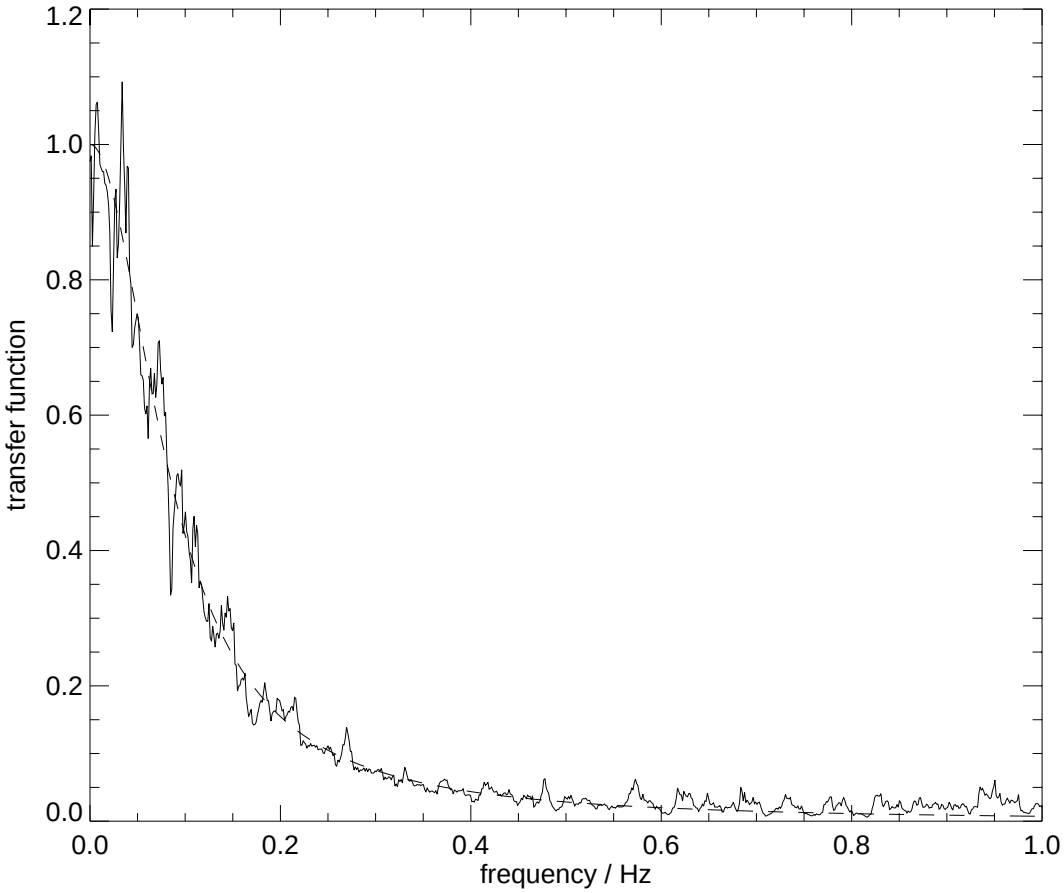

Figure 2. Transfer function for the Humitter temperature sensor calculated using data from Flight 10 (solid line) by comparing spectra from the Humitter and a high bandwidth temperature sensor (Pt wire). The dashed line shows a least squares fit of a first order time constant model (τ = 1.86 s).

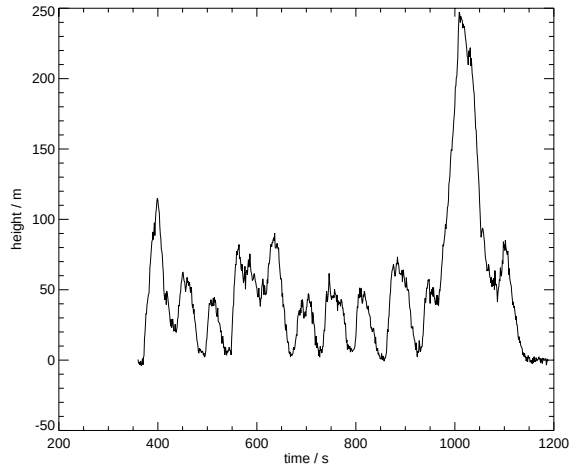

(a) Aircraft height variation during the flight.

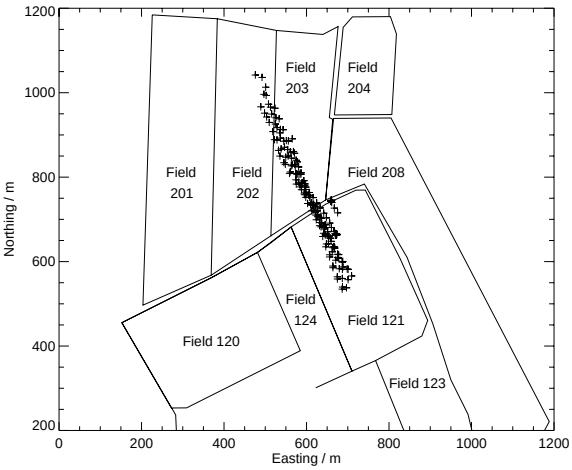

(b) Field boundaries and aircraft track (track shown only when height < 15 m, aircraft crosses boundary at 610,710).

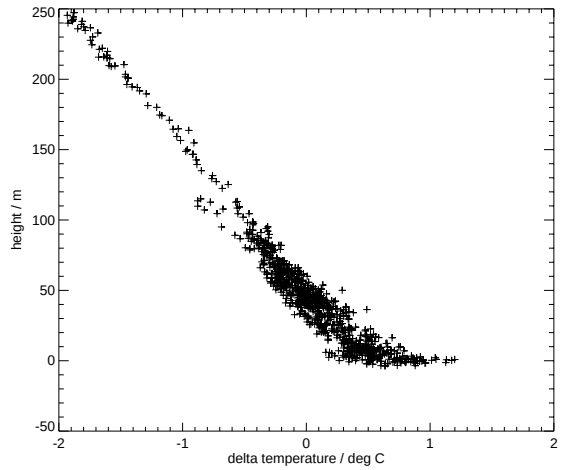

(c) Temperature variation as a function of height (relative to mean over whole flight)

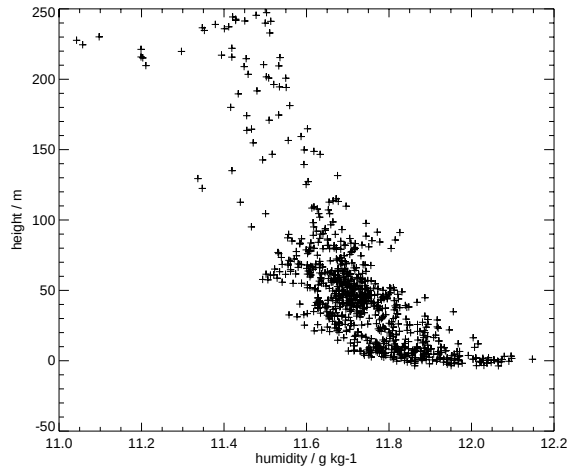

(d) Measured absolute humidity height profile

Figure 3. Flight 4 summary plots showing the aircraft's position and payload data. Subfigure (b) shows the aircraft's position relative to field boundaries. The wind was from the South-East (parallel to the plotted aircraft tracks). The boundary crossed at low level was between bare soil (Field 121, upwind) and harvested alfalfa and wheat (Fields 203,202 downwind). In subfigures (c) and (d) a point is plotted for each 0.5 s of the flight.

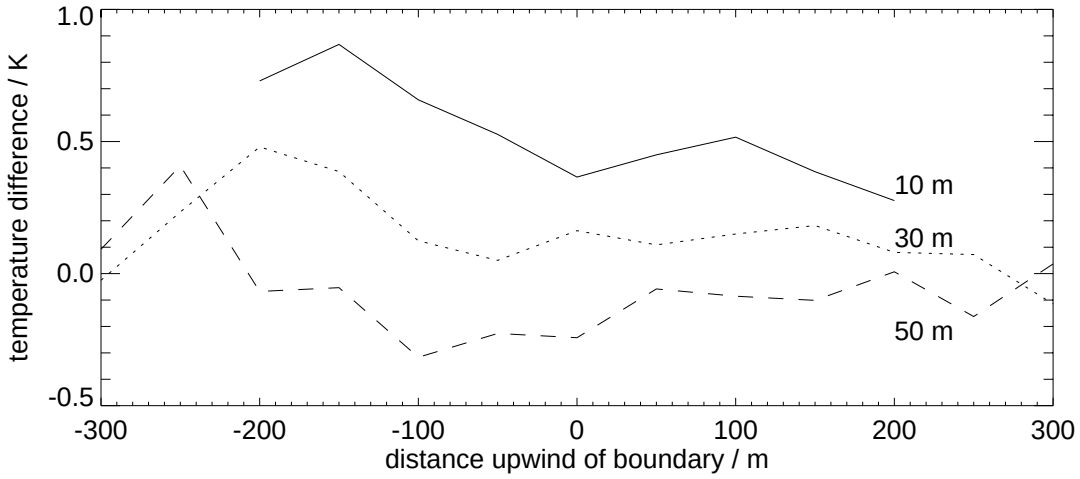

(a) Temperature relative to the mean as a function of distance upwind of field boundary at heights of 10, 30 and 50 m.

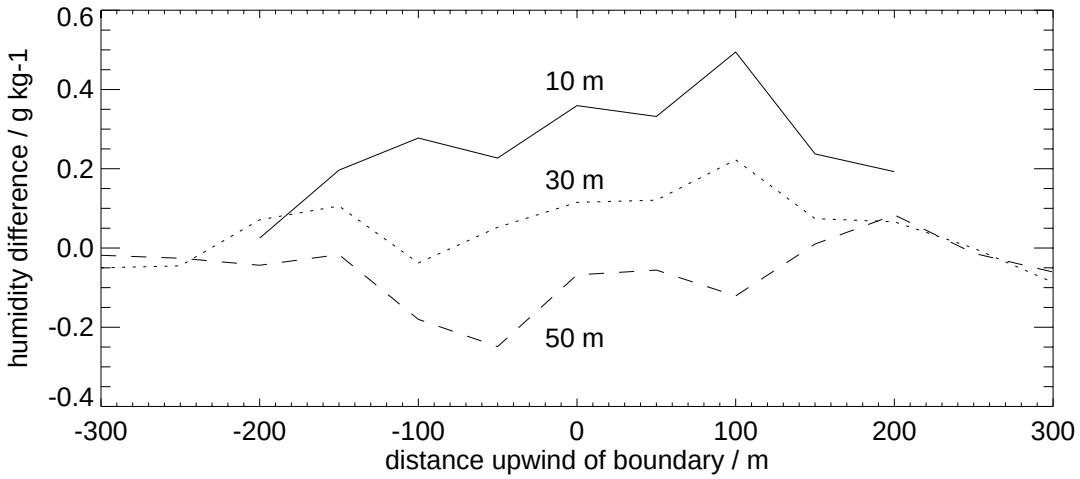

(b) Humidity relative to the mean as a function of distance upwind of field boundary at heights of 10, 30 and 50 m.

Figure 4. Horizontal profiles of temperature and humidity (averaged over 50 m horizontally and 0-20 m, 20-40 m, and 40-60 m vertically, using all available data) relative to the means during the whole of flight 9. An irrigated meadow was upwind of the boundary and a dry fallow field downwind.